

Growth, structural and optical studies on organic single crystal imidazole

P M Anbarasan¹, G Meenakshi², K Jeyapriya², M K Subramanian¹ and K Subramani¹

¹Department of Physics, Periyar University, Salem 636 011, Tamilnadu, India

²Department of Physics, K M Centre for P G Studies, Puducherry-605 008, India

³Department of Chemistry, K M Centre for P G Studies, Puducherry 605 008 India

E mail anbarasanpm@gmail.com

Received 18 April 2008, accepted 7 May 2008

Abstract Single crystal of linear optical imidazole has been grown in the laboratory by using low temperature solution growth technique. The cell parameters were determined by powder X-ray diffraction analysis. FT-Raman, FT-IR analysis were used to confirm the presence of various functional groups in the grown crystal. We have also carried out *ab initio* Hartree-Fock calculations & DFT levels invoking 6-31G(d,p) and 6-311G(2df,2p) basis sets and the results are compared with the experimental values. Thermal analysis was performed to study the thermal stability of the grown crystals. The crystals possess lower UV-cut off wavelength at 50 nm as confirmed by the transmittance study. Kurtz powder SHG measurement confirms the non-existence of non-linear property of the grown crystal.

Keywords Single crystal growth, Solution growth, FT-IR, FT-Raman, *ab initio* and DFT (Density Functional Theory), DSC technique and SHG

PACS Nos. 81.10.Dn, 42.70.Mp, 78.20.-e

1. Introduction

Crystal growth has been attracting the attention of large number of scientists from the academic and/or technological point of view. Considerable effort has been devoted to the study of this problem by means of various approaches. In the long history of these investigations physicist have been mainly interested in the spontaneous pattern of formation associated with the growth of crystals [1]. In other words, why and how in these spatially symmetric growth from the initially "Uniform" state of super cooled and/or super saturated

environment phase self organized, as observed in snow flakes [2-7] Various authors have reported much remarkable work on this topic [8-13]

Here an attempt has been made to obtain a crude picture of one particular aspect of crystal growth. Assuming an unstable configuration of crystal growth environment, we can also show how the new and transient structure (needle) comes out from the solution growth technique. A molecular crystal suitable for the usage in a number of optically linear devices required at least four basic qualities / θ it should possess high molecular induced polarisability, suitable crystallographic structure, sufficient crystal qualities and high thermal stability. The crystal structure shows a Centro-symmetric nature in the case of imidazole.

The present work reports the growth and characterization of an organic linear optical crystal imidazole with molecular formula $C_3H_4N_2$. The molecular structure of imidazole has got the hydroxyl group OH which is an electron donor. Hence the charge transfer interaction can be established which will increase the molecular polarisability. Imidazole has got a very large transmission cut-off wavelength less than 200 nm [14].

The presence of impurities definitely has influence over the properties and the growth condition of the crystal than enhancing the technological application of the material. It is well known that the paramagnetic fragrance (radical) can be trapped in a crystal matrix. Hence to understand the complete physical aspects of the grown single crystal imidazole different types of characterization analysis were made and reported here.

2. Experimental

2.1 Synthesis of Laboratory Grown Crystal

13.43 gms of glyoxal, 1.5 gms of formaldehyde in 5.26 gms of ammonia were dissolved in 15 ml of distilled water to form imidazole. This synthesis provides relatively low yields. But still it is used for forming C-imidazole.

2.1.1 Solution and Solubility

The grown imidazole has been dissolved in different organic solvents like water, benzene, ethyl acetate, acetone, ethanol and methanol. It is found that water is the best suitable solvent for growing well shaped imidazole crystal. The solution of the crystal imidazole was prepared in water and maintained at 25°C with continuous stirring to ensure homogeneous temperature and concentration over the entire volume of the solution. On reaching the saturation the content of the solution was analysed gravimetrically and this process was repeated for every 5°C. This procedure has been repeated for every temperature and a solubility curve was drawn by taking temperature along the X-axis and concentration along the Y-axis shown in Figure 1.

The curve shows that it has a high solubility and a positive solubility temperature gradient. From the solubility curve a linear variation in the temperature range of 30–50°C

is observed. Hence it is concluded that 40°C will be the optimum temperature for crystal growth in water.

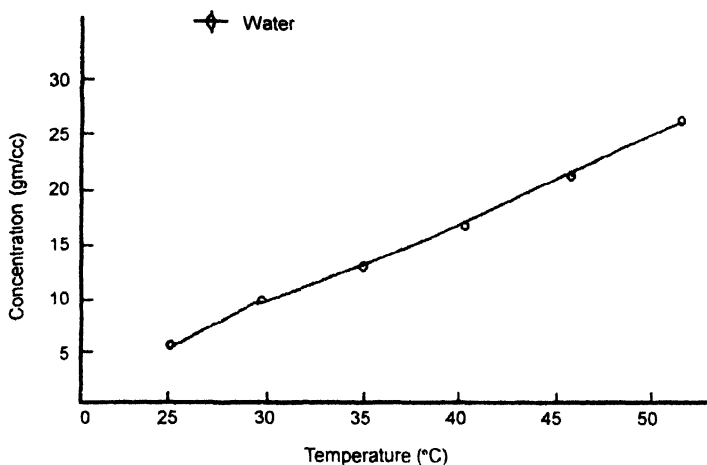


Figure 1 Solubility curve of imidazole

2.1.2 Growth of Single Crystal of Imidazole

Single crystal of imidazole has been grown by solvent evaporation technique from the saturated solution. In the present work water has been used as solvent since it was observed that when compared with other solvent crystals grown from water were well shaped. The saturated solution was prepared from water at 40°C using a temperature controlled magnetic stirrer. The solution was kept in an optically heated constant temperature bath (with temperature setting 40°C \pm 0.01°C). After repeating recrystallisation good quality of single crystal were obtained from the other solution with dimensions (7 \times 1.0 \times 0.4 mm³) approximately within a week time. The principle crystallographic axis viz a, b and c* were identified and shown in Figure 2. The photograph of grown crystal of imidazole is shown in Figure 3.

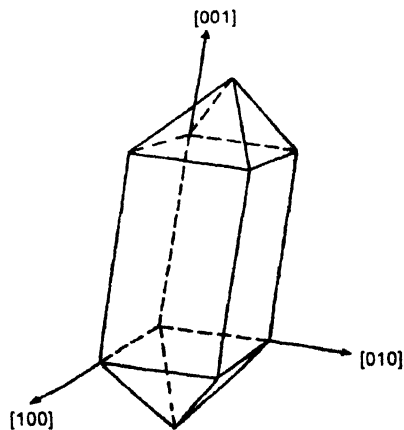


Figure 2. Morphology diagram of imidazole

The grown pure crystals without having any crack formation inside were characterized by following methods

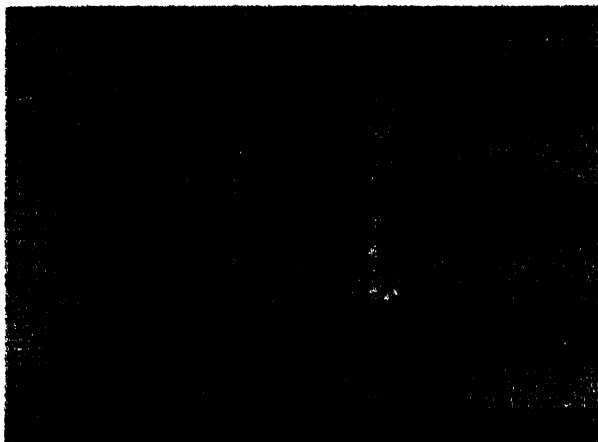


Figure 3 Photograph of grown crystal imidazole

2.2 Characterization

The unit cell constant of imidazole were determined using ENRAF-NONIUS CAD-4 single crystal X-ray diffractometer with $MoK\alpha$ ($\lambda = 0.7101 \text{ \AA}$) in $\omega/2\theta$ mode radiation to identify the structure and to estimate the lattice parameter. The crystal density was measured by floatation technique and the melting point of imidazole was found for finely powdered grown single crystal using TI-100 melting point apparatus.

The optical absorption and transmission spectra have been recorded for 2mm thickness using UV-VIS-NIR spectrophotometer of VARIAN CARY MODEL in the range 400-2000 nm as shown in the Figures 4 and 5

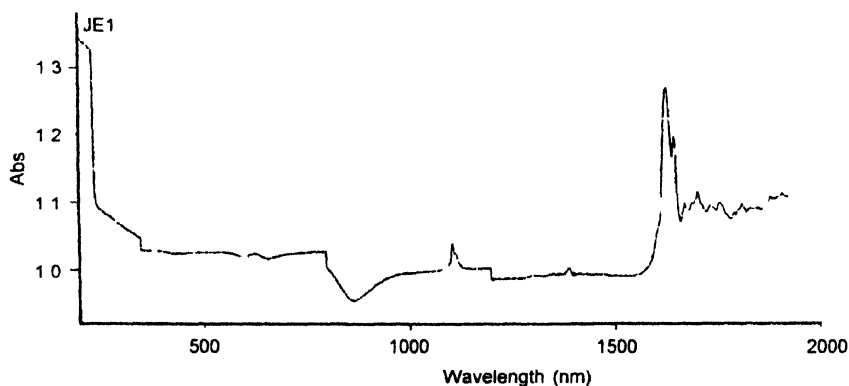


Figure 4 UV Absorptionspectrum of imidazole

FT-IR spectrum for Imidazole was recorded on Perkin Elmer FT-IR spectrometer in the range of $4000 - 400 \text{ cm}^{-1}$ following KBr Pellete technique at 300K with scanning speed of

3mm/Sec. The model of spectrum is spectrum RX-I, and its resolution 4 cm^{-1} detectors Lithium Tantalite. The FT-IR spectrum is shown in Figure 6. The FT Raman spectrum of

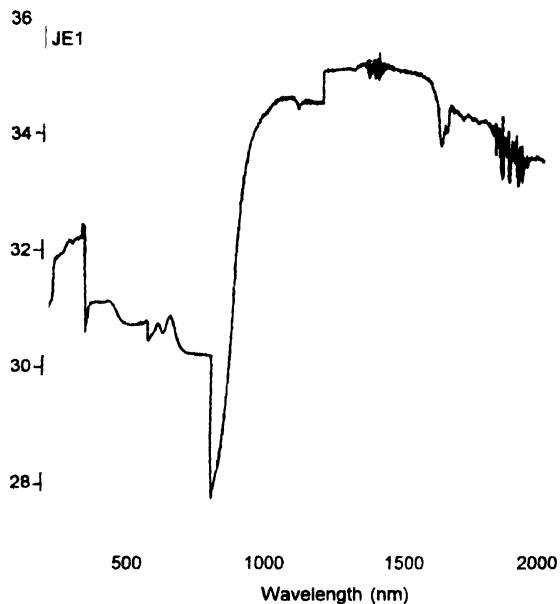


Figure 5. UV Transmission spectrum of imidazole

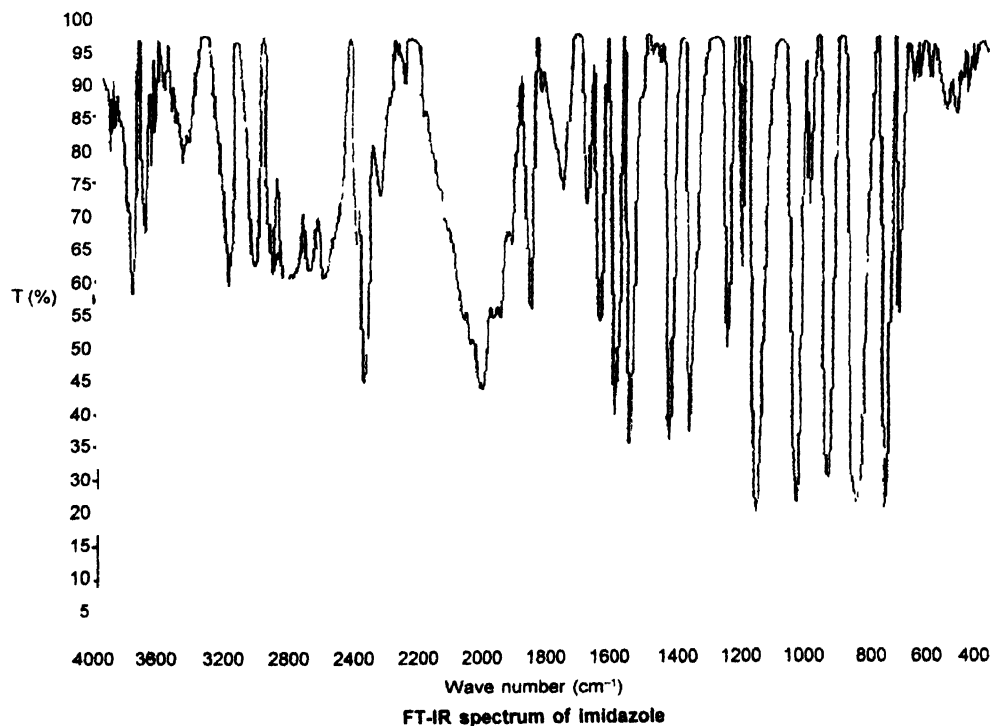


Figure 6. FT-IR spectrum of imidazole

imidazole was also recorded in the region $4000\text{--}400\text{ cm}^{-1}$ with FRA Raman module equipped with Nd YAG laser source operating at $10.6\text{ }\mu\text{m}$ line, with scanning speed of $30\text{ cm}^{-1}\text{ min}^{-1}$ of spectral width 20 cm^{-1} . The frequencies for all sharp bands were accurate to $\pm 2\text{ cm}^{-1}$. The FT-Raman spectrum is shown in Figure 7.

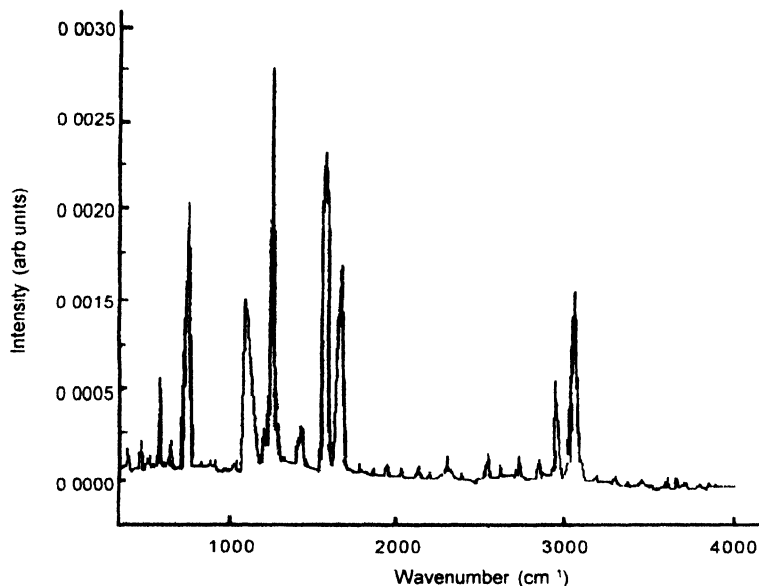


Figure 7. FT-Raman spectrum of imidazole

The thermal analysis and hardness test are carried out. Thermal behaviour of the crystallized complex was investigated by measuring Differential Scanning Calorimeter (DSC) thermogram as shown in Figure 8. The mechanical property like hardness of the crystal

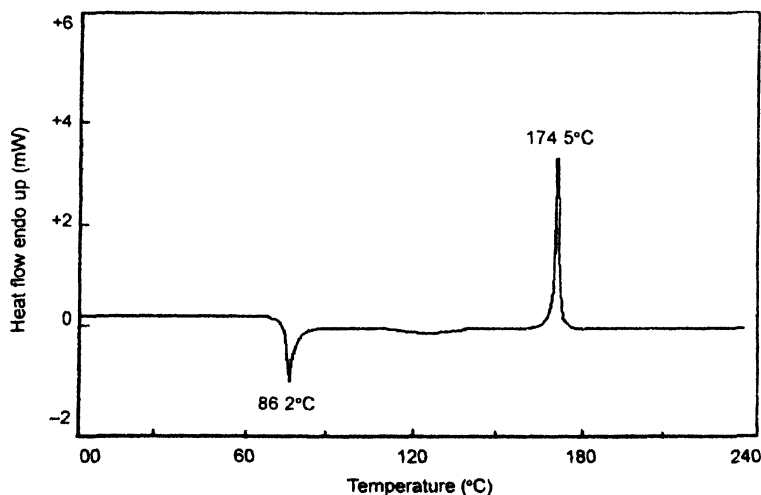


Figure 8. DSC (Differential Scanning Calorimetry) thermogram of imidazole

was studied by making indentation of (100) plane of the crystal to evaluate the Vickers's hardness number as shown in Figure 9

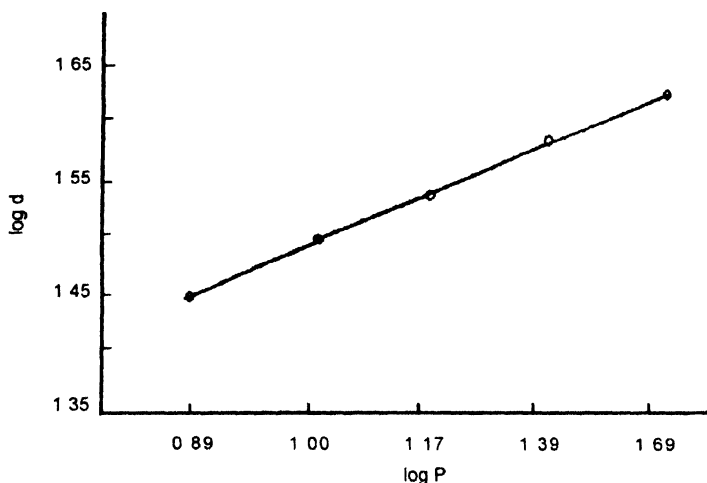


Figure 9 Hardness graph (Plot of log P vs log d) of imidazole

3 Results and discussion

3.1 X-Ray diffraction studies

The unit cell dimensions of grown imidazole were determined by single crystal X-ray diffraction technique. The system is C-face centered monoclinic with Centro symmetric space group P21/C and cell dimensions $a = 7.6806 \text{ \AA}$, $b = 5.5404 \text{ \AA}$, $c = 9.1921 \text{ \AA}$ and $\beta = 110.8404^\circ$ which agree well with the reported values [15]. The principal crystallographic axes a , b and c^* were identified and shown in Figure 2.

3.2 Measurement of density and melting point

The measurement of density is one of the most important techniques required for the study of crystal purity. The fluctuation technique is a sensitive method to determine the density of the reference [16]. The density of imidazole was calculated theoretically using the crystallization data as $\rho = 0.6 \text{ g/cc}$ which agrees well with the experimental values $\rho = 0.62 \text{ g/cc}$. A pure crystalline organic compound has in general a definite and sharp melting point, i.e. the melting point range. Therefore the melting point is a valuable criterion of purity for an organic compound. The directly measured melting point of imidazole is $89 \pm 1^\circ \text{C}$ and which is in good agreement with standard value $90 - 92^\circ \text{C}$.

3.3 Spectral and optical study

The recorded FT-IR and FT-Raman spectra for pure imidazole crystal to show the presence of fundamental groups in the crystal lattice and the observed characteristic vibrational bands were assigned [Table-1]. In order to obtain a more complete interpretation of the vibrational spectrum and to determine the degree of normal modes, by combining the

Table 1. Observed and calculated FTIR and FT-Raman frequencies (cm^{-1}) and assignments for imidazole by *ab initio* Hartee-Foch and density functional methods (Species A/B)

Observed frequencies (cm^{-1}) and intensity		Calculated frequency (cm^{-1})	Assignment
Laser Raman	Infrared		
3788W	3801M	3807	Hydrogen bonded stretching vibrations
3398VW	3409VW	3456	N-H asymmetric stretching vibration
3306W	3295W	3302	C-H asymmetric stretching
3108W	3111W	3109	N-H symmetric stretching
3061S	3048M	3052	-C-H symmetric stretching
2997VW	2989W	2969	N-H out-of plane bending
2904VW	2897W	2919	C-H stretching superimposed with N-H stretching
2871VW	2790W	2861	N-H group stretching vibrations
2699VW	277W	2755	Strongly bonded hydrogen vibrations
2701VW	2615W	2611	N-H deformation combination bands
2388M	2381VS	2398	Overtone and combinations
2933W	2055M	2061	Double bonded stretching vibrations
2007W	2015S	1995	N-H stretching group vibrations
1799W	18048W	1871	=C-H out of plane bending
1701W	1698W	1709	C=N symmetric stretching
1678W	1683W	1666	C=C asymmetric stretching
1609S	1614S	1602	N-H torsion
1576M	1590S	1589	C=C asymmetric ring stretching
1517VW	1510VW	1508	C=C symmetric stretching
1449M	1466S	1459	C-N asymmetric stretching
1413M	1396S	1403	C-H in-plane bending
1387W	1392S	1368	C-N symmetric stretching
1249VW	1265W	1259	C-N-H stretching
1198VS	1212S	1202	N-H in-plane bending
1098S	1092S	1085	N-H twist
998M	987VS	1005	C-H in plane bending
989VW	976 VW	953	C=C torsional
896S	910S	905	C-H out of plane bending
865VS	873VS	877	N-H out-of plane bending
856VW	877VW	854	C-H deformation
793VW	789VW	800	N-H wagging
731VS	721VS	715	C-H out of plane deformation
629W	631M	620	C=C out of plane bending
578W	563W	551	C-N out-of plane bending
439VW	462VW	453	N-H torsional oscillation

VS – Very Strong, S – Strong, M – Medium, W – Weak, VW – Very Weak

results of the GAUSSVIEW program with symmetry considerations, along with available related data, vibrations frequency assignments were made with high degree of accuracy FT-Raman, FT-IR analysis was used to confirm the presence of various functional groups in the grown crystal. We have also carried out *ab initio* Hartree-Fock calculations & DFT levels invoking 6-31G(d,p) and 6-311G(2df, 2p) basis sets and the results are compared with the experimental values [17]

3.3.1 C = C vibrations

The C = C vibrations are observed to the bands at 1683, 1590, 1510, 976, 631 cm^{-1} and 1678, 1576, 1517, 989, 629 in FTIR and FT-Raman spectra respectively. The C = C stretch can readily be assigned to the medium band in the Raman spectrum at 1576 cm^{-1} . The FTIR counter part for this mode has been identified at 1590 cm^{-1} . Three other skeletal modes containing significant contributions of C = C stretching are also assigned to the bands at 1130, and 1001 in FTIR, 943 and 925 cm^{-1} are observed in the Raman spectrum, respectively. The calculated values using with GAUSSVIEW programme for C = C vibrations are 1666, 1589, 1508, 953, 620 cm^{-1} .

3.3.2 C–N vibrations, C = N vibrations

The identification of the C–N stretching frequency in the imidazole is a rather difficult task since there are problems in identifying these frequencies from other vibrations. FTIR spectrum observed the C–N stretching band at 1466, 1392, 1265 (C–N–H), 563 cm^{-1} in imidazole identified the stretching frequency of the C – N bond at 1701 cm^{-1} in FT Raman counter part for this modes has been assigning the bands at 144, 1387, 1249, 578, cm^{-1} corresponding to C – N and C – N stretching, respectively. The calculated values of C – C vibrations are 1709, 1459, 1368, 1259, 551 cm^{-1} .

3.3.3 C–H vibrations

C–H vibrations in the region 3043–3078 are in agreement with experimental assignments 3040–3106 cm^{-1} . The C–H in plane bending vibrations assigned in the region 1403–1005 cm^{-1} while the experimental observations are at 3306, 3061, 1413, 998, 896, 856, 713 cm^{-1} and at 3195, 3048, 2898, 1396, 987, 910, 877, 721 in FTIR and FT-Raman spectra, respectively. The calculated frequencies of C–H vibrations are 3302, 3052, 2919, 1403, 1005, 905, 854, 715 cm^{-1} .

3.3.4 N–H vibrations

There are twelve bands are identified for the N–H vibrations in the imidazole and in the FTIR spectrum, it is assigned to the band at 3409, 3111, 2989, 2790, 2615, 2015, 1614, 1212, 1092, 873, 787, 462 cm^{-1} and in the FT-Raman spectrum, it is observed at 3398, 3108, 2997, 2871, 2701, 2007, 1609, 1190, 1098, 865, 793, 439 cm^{-1} . The N–H inplane bending and N–H out-of plane bending are calculated at 1202 cm^{-1} and 715 cm^{-1} , which agree well with literature value [Sundaraganesan *et al*]

Kurt SHG test was performed to find the non-linear optical property of imidazole. The measurement confirmed the non-existence of non-linear property of the grown crystal. The SHG of grown imidazole single crystal sample was not observed by subjecting the grown imidazole crystal to Spectra – Physics Quanta-Ray DHS2 Q-switched Nd YAG laser radiation emitting a fundamental wavelength of 1064nm with pulse width of 10ns.

From Figures 6 & 7 of optical absorption and transmission spectra, it is observed that the cut off wavelength is found to be 50 nm that is comparable with the earlier values [14].

3.4 Thermal Analysis

The heat capacity at constant pressure C_p of grown imidazole single crystal was measured by DSC analysis in the temperature range (30°C/10.00(K/min) / 400°C). This method reveals a sharp endothermic peak at 86.2°C and an exothermic peak at 174.5°C. The endothermic transient is attributed to the presence of un-coordinated alcohol group in this structure, since the alcoholic group is known to exhibit a melting point between 89–91°C. The exothermic peak could be attributed to the decomposition of the substance imidazole. To calibrate the system within 2%, indium specimens were used. Powdered samples of imidazole with purity of 99.99% as determined by vapour phase chromatography were placed in a sealed aluminium differential scanning calorimetric pan. The DSC curve of imidazole is shown in Figure 8. The specific heat of imidazole at 298K was found to be $2.754 \text{ Jg}^{-1}\text{K}^{-1}$.

3.5 Hardness

The Vicker's hardness value was measured by using the formula,

$$VHN = \left(\frac{P}{A} \right) = \left(\frac{2P \sin \frac{\theta}{2}}{d^2} \right) = 18544 \frac{P}{d^2} \text{ kg/mm}^2 \quad (1)$$

and the value is found to be 85 kg/mm^3 . Figure 9 shows the load versus Vicker's hardness number for imidazole crystal. At lower load it is observed that the increase of load increases the hardness. This is due to the work hardening of the surface layers. Beyond the load of 50 grams a significant crack will occur. This may be due to the release of internal stress generated by indentation. Using this study the nature of the substance (harder or softer) can be identified.

4. Conclusion

The imidazole crystal has a very large transmission range which will be useful for wide application, like, obtaining Raman coherence source spectroscopic real time analysis holography, ultra high speed optical gate amplifiers, Choppers etc. The crystal structure is stabilized by hydrogen bonding. We have carried out *ab initio* and density functional

theory calculation on the structure and vibrational spectrum of imidazole. Comparison between the calculated and experimental structural parameters indicates that B3LYP are in good agreement with experimental ones. Vibrational frequencies, infrared intensities and Raman activities calculated by B3LYP/6-311G(2df,2p) method agree very well with experimental results. This study demonstrates that scaled DFT/B3LYP calculations are a powerful approach for understanding the vibrational spectra of organic single crystal imidazole.

The elucidation of molecular structure from FT-IR and FT-Raman studies confirmed the purification of the crystal. The growth rate is high along C-axis. The thermal behaviour of imidazole studied by DSC supported the structure suggested.

Acknowledgments

The authors are very thankful to Dr S. Moorthy Babu, Crystal Growth Centre, Anna University, Chennai-25 and Dr N. Sundaraganesan, Department of Physics (Engg.), Annamalai University, Annamalai Nagar – 608 002, India, for the use of Laboratory and software facilities respectively. The authors are also deeply indebted to the anonymous reviewers for their constructive and helpful comments.

References

- [1] J. S. Langer *Rev. Modern Physics* **52** (1980)
- [2] U. Nakaya *Snow crystals* (Cambridge MA: Harvard University Press) (1954)
- [3] P. V. Hobbs *Ice Physics* (Oxford: Clarendon Press) ch 8 (1974)
- [4] T. Kobayashi *Phi. Mag.* **6** 1363 (1961)
- [5] J. Hallett and B. J. Mason *Proc. Roy. Soc. (London)* **A247** 440 (1958)
- [6] T. Kuroda *Kinetik des Eiswachstums aus der Gasphase Und seine Wachstumsformation*. Thesis TV Braunschweig (1979)
- [7] T. Kuroda *J. Crystal Growth* **56** 189 (1982)
- [8] J. S. Langer and H. Muller-Krumbhaar *Acta Met.* **26** 1681 (1978)
- [9] J. S. Langer and H. Muller-Krumbhaar *Acta Met.* **26** 1689 (1978)
- [10] J. S. Langer and H. Muller-Krumbhaar *Acta Met.* **26** 1697 (1978)
- [11] W. Lodfield *Mater. Sci. Eng.* **11** 211 (1973)
- [12] E. G. Holtzmann *J. Appl. Phys.* **41** 1460 (1970)
- [13] E. G. Holtzman *J. Appl. Phys.* **41** 4769 (1970)
- [14] S. Dhanuskodi and S. Manikandan *Ferroelectrics* **234** 183 (1999)
- [15] Li Zhengdong, Su Geno and Wu Baichang *J. Crystal Growth* **121** 516 (1992)
- [16] A. F. Loffe *Phys. Stat. Sol.* **116** 457 (1989)
- [17] N. Sundaraganesan, B. Dominic Joshua and K. Settu *Spectrochimica Acta Part A* **66** 381 (2007)